Optical illusion shape texturing using repeated asymmetric patterns

Citation	Chi, M. T., Yao, C. Y., Zhang, E., & Lee, T. Y. (2014). Optical illusion shape texturing using repeated asymmetric patterns. The Visual Computer, 30(6-8), 809-819. doi:10.1007/s00371-014-0989-3
DOI	10.1007/s00371-014-0989-3
Publisher	Springer
Version	Accepted Manuscript
Terms of Use	http://cdss.library.oregonstate.edu/sa-termsofuse

CGI2014 manuscript No.
(will be inserted by the editor)

Optical Illusion Shape Texturing using Repeated Asymmetric Patterns

Ming-Te Chi · Chih-Yuan Yao · Eugene Zhang · Tong-Yee Lee

Abstract Illusory motions refer to the phenomena in which static images composed of certain colors and patterns lead to the illusion of motions. This paper presents an approach to generating illusory motions on 3D surfaces which can be used for shape illustration as well as artistic visualization of line fields on surfaces. Our method extends previous work on generating illusory motions in the plane, which we adapt to 3D surfaces. In addition, we propose novel volume texture of Repeated Asymmetric Patterns (RAPs) to visualize bidirectional flows, thus enabling the visualization of line fields in the plane and on the surface. We demonstrate the effectiveness of our method with applications in shape illustration as well as line field visualization on surfaces. For the design of optical illusion art, it is a tough case to arrange the distribution of RAP. However, we provide a semi-automatic algorithm to help users design flow direction. Finally, this technique applies to the design of street art and user could easily set the perspective effect and flow motion for illustration.

Keywords illusory motion · line field · Repeated Asymmetric Patterns (RAP) · optical illusion art

Ming-Te Chi
National Chengchi University. E-mail: mtchi@cs.nccu.edu.tw

Chih-Yuan Yao
National Taiwan University of Science and Technology.
E-mail: cyuan.yao@csie.ntust.edu.tw

Eugene Zhang
Oregon State University. E-mail: zhange@eecs.oregonstate.edu

Tong-Yee Lee
National Cheng-Kung University. E-mail: tonylee@mail.ncku.edu.tw

1 Introduction

In this paper we present to our knowledge the first general technique to produce *illusory motions* on 3D surfaces (Figure 1). By illusory motions we are referring to the phenomena in which motions can be perceived from static images through the use of *designed* contrasting color patterns. Chi et al. [2] provide an efficient and general computational framework to generate *self-animating images*, a well-known and fascinating form of illusory motions invented by Kitaoka [3], for any given vector field in the plane. Their framework not only produces exciting artwork from an input image such as van Gogh's *Starry Night*, but also provides a novel vector field visualization technique that requires only *static* images yet still can convey the *dynamic* nature of the flows.

Optical art (OP art) is a visual art that makes use of optical illusions, first appeared in 1965. Many well-known works are designed by artist and psychologist. Figure 2 shows two famous art works which attempt to provide a sense of 3D shapes with color patterns in the plane. Recently, in computer graphics area, Ingils et al. [11] proposed an OP art generation method converted from a 2D bi-tonal image. These works inspired us to propose a system to convert a 3D mesh to an art illustration with optical illusion effect.

Generating consistently perceivable illusory motions on manifold surfaces from static images is the goal of this paper, which is motivated by the following: First, artistic rendering of 3D surfaces is one of the fundamental goals for computer graphics, and illusory motions on surfaces can provide such a means. Second, shape illustration can deliver a concise representation of surfaces often used in computer-aided design and manufacturing as well as technical illustration. Illusory motions, when following salient features, can help

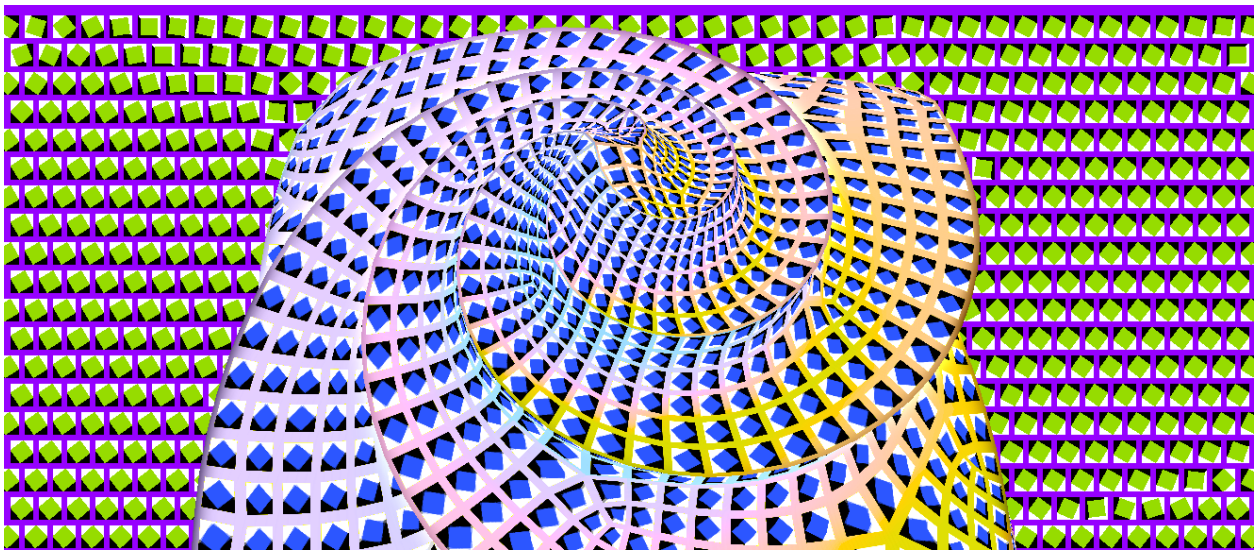

Fig. 1 An artistic illustration of the Flower model using feature-aware illusory motion, generated with our technique.

convey the shape of the surfaces without the need for any animated media.

Despite the potential benefits of illusory motions in graphics, geometry processing, and visualization, there are a number challenges to adapt the techniques to surfaces. First, placing color patterns on surfaces is more difficult than on the plane due to the topological and geometric constraints associated with surfaces, such as handles, protrusions, and folds. These constraints can impact the strength of the perceived motions due to the depth, viewing angle, and self-occlusion on the surface. Second, natural line-based features on the surfaces, such as the principal curvature directions as well as ridges and valleys, are intrinsically bidirectional, i.e., a two-way street. In contrast, the method of Chi et al. [2] only applies to vector fields, which has a clear forward and backward direction, i.e., a one-way street. Treating a line field (bidirectional) as a vector field (unidirectional) can lead to visual artifacts such as artificial discontinuities and the loss of singularity patterns [32].

To address these difficulties, we develop a framework that effectively generates color patterns on a surface to achieve the desired illusory motion. Our contributions are:

1. We extend the technique of Chi et al. [2] to handle line fields, such as principal curvature tensors and the ridge and valley lines. We achieve this by developing novel RAPs to visualize bidirectional. We provide an optimized view-dependent flow adjustment method to maximize RAP illusory movements in the image space.

2. We further enhance the perception of motions by placing contrasting RAPs in the background pixels in the image plane, applying shading to RAPs, and incorporating existing image enhancement techniques during post processing.

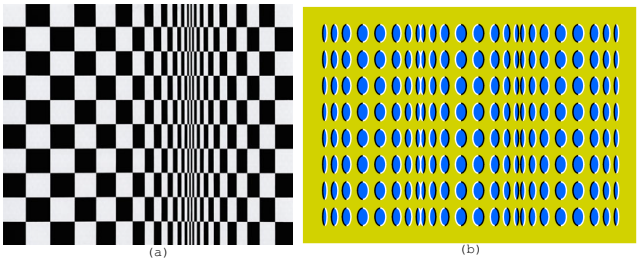

Fig. 2 Optical illusion art. (a) Movement in Squares, by Riley (1961). (b) Rollers, by Kitaoka (2004).

We have applied our technique to a number of applications, such as surface decoration, shape illustration, and line field visualization on surfaces.

The remainder of the paper is organized as follows. In Section 2 we review existing research mostly relevant to this work. We then provide an overview of our system in Section 3 and describe the details of each step in Section 4. We show our results in Section 5 summarize and discuss possible future research avenues in Section 6.

2 Previous Works

Non-photorealistic rendering (NPR) of surfaces: There has also been some recent work on visualizing cross fields (4-RoSy) on surface using an extension of line integral convolutions on NPR illustration of surfaces, such as line drawings and hatching [10, 4, 12, 16] and non-photorealistic shading [17]. There has also been extensive research in texture

and geometry synthesis on surfaces as a means of decorating geometry [28,26,18,19]. Our method differs from all this work in that we provide an artistic illustration of surfaces through the use of illusory motions from static images.

Motion cues and illusory motions: Using motion cues for the shape perception, so-called "structure-from-motion", has long been studied in psychology [5,24]. Lum et al. [21] visualize a surface by generating particle flows on the surface using dynamic media. While we also use motion cues for shape depiction, our method does not require dynamic media. Kitaoka and Ashida [15] suggest that the combination of certain color patterns can produce strong peripheral drift illusions. Gossett and Chen [9] have experimented with the creation of illusory motions by self-animating line textures. Wei [27] proposes an automatic method to visualize vector fields using tile-based RAPs. Chi et al. [2] propose an automatic streamline- and RAP-based method to generate self-animating images. All of the previous work has focused on generating illusory motions in the plane.

3 Overview

In this section we discuss the challenges on surfaces as well as provide an overview of our system. The method of [2] can efficiently handle planar vector fields. Adapting it to surfaces with line fields has the following added difficulties:

1. Intrinsic directions in surfaces, such as ridges, valleys, and principal directions, are bidirectional. As demonstrated in [10,7,32], these features are best represented as second-order symmetric tensors. In contrast, RAPs are unidirectional by design, i.e., vector fields. Converting a tensor field into a vector field can lead to discontinuity in the resulting vector field [32,23].
2. Even when visualizing a line field on surfaces, it is not a trivial task to place RAPs so that patterns similar to the planar case [2] can be generated. One of the fundamental reasons behind this is the lack of a high-quality quadrangulation for surfaces with complex geometry.

To address these difficulties, we propose a novel algorithm in the following pipeline. First, we generate a quadrilateral remesh for the arbitrary triangular meshes, each of whose quads (or cells) in the remesh will be textured with a RAP. The quadrilateral mesh is generated using the method of [25] which is known to produce high-quality quad meshes. Also during this step, the salient curves on the surface are either extracted through automatic techniques such as [31].

In the second step, we generate a directional field on the surface that respects the salient curves obtained in the first step. This directional field can be a vector field or a line field. In the case of a line field, it is converted into a piecewise continuous vector field where the discontinuity in the vector field occurs mostly on the salient features. Our experiments show that this method can help increase the contrast between neighboring regions, thus leading to a strong perception of the shape.

Next, we design and select appropriate RAPs based on the type of the aforementioned directional fields and arrange them in the elements of the quad mesh. This is further enhanced with a view-dependent, optimized flow adjustment step which tends to maximize the perceived illusory motion in the image space.

Finally, the rendered image is enhanced by generating a background flow, adding shading, texture mapping, and applying image enhancement. Figure 3 shows part of the pipeline (without shading, image enhancement, and background vector field).

4 Algorithm

In this section, we provide the details of our pipeline, namely, directional field generation from salient features on the surface, RAP design and placement on surfaces, and enhancement techniques during post processing.

4.1 Curve-Guided line Field Generation

To better illustrate the shape of an object, we generate a smooth and shape-revealing RAP flow on the object according to a second-order symmetric line field derived from the surface. The major eigenvectors of this line field can be used to describe principal curvature directions often used in hatching as well as ridges, valleys, and demarcating curves typically used in line drawing of shapes. More specifically, by a *tensor* we mean a 2×2 matrix t_{ij} that is both *symmetric* ($t_{12}=t_{21}$) and *traceless* ($t_{11}+t_{22}=0$). Such a tensor can be rewritten as $\rho\begin{pmatrix}\cos 2\theta & \sin 2\theta\\ \sin 2\theta & -\cos 2\theta\end{pmatrix}$ where $\rho=\sqrt{t_{11}^2+t_{12}^2}$ is the tensor magnitude and $\theta=\frac{1}{2}\arctan(\frac{t_{12}}{t_{11}})$ encodes the eigenvector information.

Each salient curve is a polyline consisting of edges in the mesh. First, we compute a tangential tensor at each interior vertex on the curve. This is achieved by generating a 2×2 symmetric traceless tensor on each of the two edges incident to the vertex, projecting the tensors onto the vertex's tangent plane, and averaging them. To generate the aforementioned tensor on an edge, we simply choose the tensor (up to normalization) whose major eigenvectors are parallel

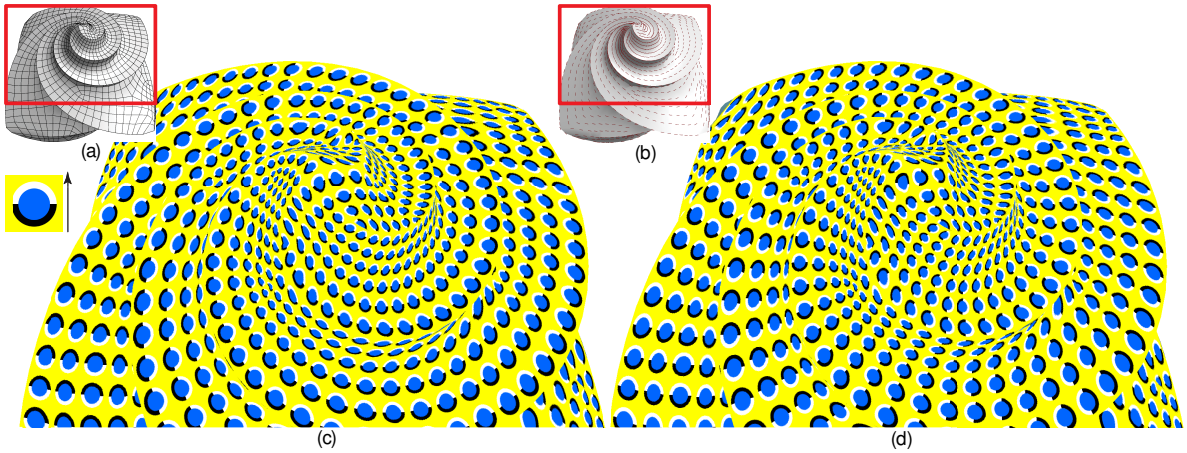

Fig. 3 An overview of part pipeline overview for shape depiction (without enhancement in background and shading): (a) quad-mesh generation and salient curve extraction, (b) curve-guided directional field generation, (c) RAP tiling, and (d) flow adjustment.

to the edge. Finally, these tensors are propagated from the salient curves to the rest of the surface as follows.

Along a salient line, each sample point $\mathbf{p}_0$ and a tangential 2×2 symmetric tensor $T(\mathbf{p}_0) = \begin{pmatrix} t_{11}(\mathbf{p}_0) & t_{12}(\mathbf{p}_0) \\ t_{12}(\mathbf{p}_0) & -t_{11}(\mathbf{p}_0) \end{pmatrix}$ whose major unit eigenvectors specify the desired orientation at $\mathbf{p}_0$, such as the Figure 4 shown. Together, the set of all salient features provide the boundary conditions to the following Laplace equations:

$$\begin{pmatrix} \bigtriangledown^2 t_{11} = 0 \\ \bigtriangledown^2 t_{12} = 0 \end{pmatrix} \tag{1}$$

in which $\bigtriangledown^2$ is the discrete Laplace operator [32]. Note that both t_{11} and t_{12} are entries of a tangential tensor field. Consequently, to compute $\bigtriangledown^2_T(\mathbf{p}_0)$ one needs to perform *parallel transport* of the eigenvectors from any neighboring vertex of $\mathbf{p}_0$ along the shortest geodesic connecting them. Our method of setting up and solving Equation 1 follows closely that of [22], to which we refer the readers for implementation details.The major eigenvectors of the propagated tensor field will then be used to guide RAP placement on the surface.

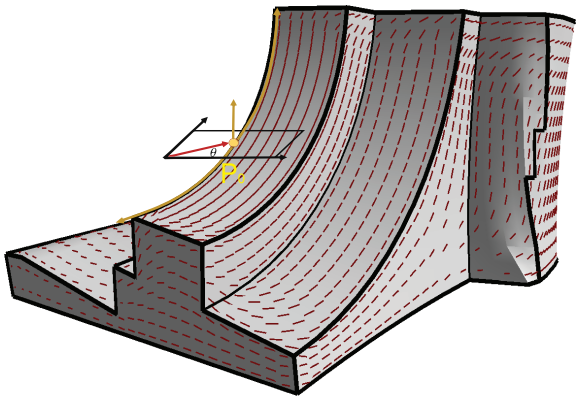

Fig. 4 P_0 is the sample point on the salient line and we could compute the corresponding tangent plane by its normal direction. Then, we could calculate angle, θ, to construct tensor matrix.

4.2 RAP Design and Placement

RAP Placement: To visualize vector fields on our quad meshes, we make use of the original RAPs developed by Kitaoka and Ashida [15]. We have observed that these patterns work efficiently on surfaces despite the distortion introduced by viewing conditions such as field of view and depth. We hypothesize that this is due to the fact that familiar size of RAP with perspective distortion is an important monocular cues in ***depth perception***. Note that the idea has led to various applications in Optical Art as shown Figure 2. Leveraging on depth perception, we use RAP-tiles with a constant shape to texture the faces in the quad mesh. The RAPs that we employ in this research are of TYPE IIa based on the classification of the optimized Fraser-Wilcox illusion [14]. In this setting, the cycling of a black-blue-white-yellow pattern can provide strong illusions of unidirectional motion in the peripheral and near-peripheral vision (Figure 3(c): the arrow next to the RAP is only for the purpose of annotating the direction of the perceived motion). Due to the resolution limit, we recommend the readers zoom-in on the results shown in the paper to better perceive illusory motion. We also refer to the supplementary materials accompanying this paper for more high-resolution images.

When visualizing a tensor field, the aforementioned RAPs become inadequate since a tensor field has two directions at any given point except the degenerate points where the tensor is isotropic. Zhang et al. [32] point out that converting a tensor field into a vector field by choosing one of the two directions leads to artificial discontinuity in the re-

sulting vector field. A similar problem exists for 4-RoSy fields, except that it is even more pronounced since there are four directions at any non-degenerate points. Our strategy to handle this is two-folds. First, we develop a new RAP pattern that can illustrate both directions for a tensor field or four directions in a 4-RoSy field. Second, when converting a tensor or 4-RoSy field into a vector field, we carefully choose the directions at each cell in the mesh such that directional discontinuity after the conversion mostly occur along salient curves. We have observed that discontinuity along such curves can in fact enhance the perception by the viewer.

RAP Design: To take advantage of the parametrization of quadrilateral mesh, we design a quad-like RAP as Figure 5(b), that can fully use the space in the cell of quadrilateral mesh and also depict the flow of parametrization. Furthermore, we can recursively add RAP inside a RAP as Figure 5(c). Care must be taken about the quad-like RAP to enhance the strength of illusion. The circle-like RAPs can easily rotate along the line field, but the quad-like RAPs must be generated for each direction to maintain the color order of black-blue-white-yellow. To avoid RAP computation in rendering, we generate 36 different patterns for every 10 degree to build a volume texture in preprocess, and select the desired pattern according to the direction of quad in rendering time. In Figure 5 (b), (c) and (d), each row presents the pattern with same direction in each 3D texture.

When visualizing a tensor field, it is natural to strive for new types of RAPs that can simultaneously produce two flows with opposing directions. One possible approach is to place two opposite, unidirectional RAPs in a single quad. Unfortunately, we have found this to be ineffective since the opposing flows is too close and tend to neutralize. To address this difficulty, we adapt existing RAPs to simultaneously deliver the unidirectional illusory motion as well as bidirectional information in a tensor field. Note that each of the four colored regions in a RAP must be clearly perceived in order to induce a strong illusion. Consequently, we avoid placing multiple RAPs in a quad. Instead, we design a RAP with a four-fold rotational symmetry to provide bidirectional information as shown in Figure 5(d). This RAP uses a diamond shape (the blue region) to express the 4-Rosy information but can still result in a unidirectional motion which is one of the two directions.

Flow Adjustment: The new RAPs are asymmetric due to the relative locations of the white and black regions in the RAP. This means that we still face the task of choosing a direction out of the two possible directions for a tensor and four for a 4-RoSy. Chi et al. [2] have found that the illusory motions are more likely to be perceived along curves where the vector field has opposite orientations across the curve. This observation motivated our approach in converting a tensor or 4-RoSy field into a vector field. We divide the domain into regions based on the salient curves, and choose consistent orientations inside each region while maximizing inconsistencies across boundaries between neighboring regions. Specifically, the directions from two sides of a point on the salient feature will be opposite to each other in the tensor case. For cross fields, the two vectors will be related by a rotation of 90, 180, or 270 degrees. This angle deficit along any boundary between two regions is further required to be constant.Note that our region segmentation is performed in the image space, so is the process of selecting a directional vector from a tensor or 4-RoSy field.

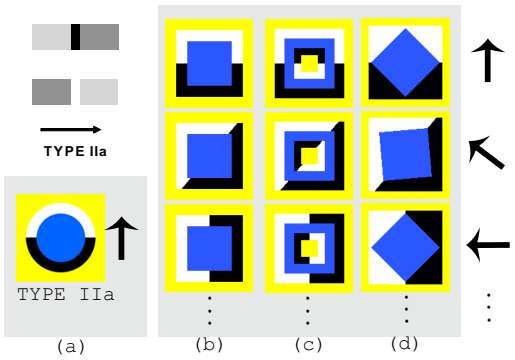

Fig. 5 RAPs configurations: (a) two RAPs design by Kitaoka; (b), (c) and (d) are selected RAPs from the precomputed volume texture. In each row, the arrow indicates the direction of illusory motion.

Specifically, given a viewpoint, the model is rendered with flat shading and the surface fields are projected onto the image plane. Based on similarity of vector fields and all constrained lines, we use a simple floodfill method to segment the rendered model into several regions. We construct an adjacency graph $\mathbf{G} = \{\mathbf{V}, \mathbf{E}\}$ where the nodes in $\mathbf{V} = \{\mathbf{v}_1, \mathbf{v}_2, ..., \mathbf{v}_n\}$ each corresponds to a region in the segmentation. The edges in $\mathbf{E}$ records the adjacency relationship among the regions.

Our goal is to choose directions for each region such that they are discontinuous across region boundaries but as continuous as possible within reach region. There are two types of discontinuities: (a) opposite flow directions, and (b) mutually perpendicular flow directions. We have found that it is not always possible to produce discontinuities between any pair of neighboring regions, especially in the case of tensor fields when there is only one type of discontinuity (opposing flows). Consequently, we need to decide where to place discontinuity when a global solution does not work. This is achieved by assigning a weight $\mathbf{w}_b$ to each edge, $e = (v_i, v_j) \in \mathbf{E}$.

$$w_b(\mathbf{v}_i, \mathbf{v}_j) = \alpha l_{ij} N_{ij} + \beta A_{ij} \tag{2}$$

where l_{ij} is the length of the shared boundary between two connected segmented regions, N_{ij} is the total dot product between the regions along the boundary curve, and $A_{ij} = area(\mathbf{v}_i) + area(\mathbf{v}_j)$ is the total area of the two regions. Both l_{ij} and $Area_{ij}$ tend to favor regions with a large combined area and/or a long common border. Unlike [2], we consider N_{ij} which favors the assignment of inconsistent flows to adjacent regions across a high curvature boundary.

Once the adjacency graph $\mathbf{G}$ is constructed, we simplify $\mathbf{G}$ using edge collapses with the edge cost function being $\mathbf{w}_b$ [6]. Given any two adjacent regions, if $\mathbf{w}_b$ of the corresponding edge $\in \mathbf{E}$ is below a threshold, their corresponding nodes $\in \mathbf{G}$ will be merged and no inconsistent flows will be attempted between them. Finally, similar to [2], we maximize the following energy E_{graph} of this simplified adjacent graph $\mathbf{G}' = (V', E')$ by using the following two-coloring graph algorithm.

$$E_{graph} = \sum_{v'_i \in V'} \sum_{v'_j \in \mathscr{N}(v'_i)} w'_b \cos^{-1}((\alpha_i Dir_i) \cdot (\alpha_j Dir_j)) \tag{3}$$

$$\alpha_i = \begin{cases} +\mathbf{1}, \text{ black.} \\ -\mathbf{1}, \text{ white.} \end{cases} \tag{4}$$

where $\mathbf{V}' \in \mathbf{G}'$, $\mathscr{N}(v'_i)$ is the 1-ring neighborhood of $\mathbf{v}'_i \in \mathbf{V}'$, Dir_i and Dir_j denote a representative direction of the vector fields in two corresponding segmented regions i and j. We use $alpha_i$ to indicate the color state in Equation (4): black color is for preserving the direction and white color for reversing it. We can apply the above adjustment procedure to generate opposite flows in neighboring regions according to the type of the directional field.

4.3 Enhancements

Even the RAPs are well designed and placed on surfaces, the motion effect may be still weak. We use the following techniques to enhance the perception. First, we can strengthen the illusion by generating an opposite RAP flow in the background. Second, we can optionally apply some extra shape cues to complement the lost information by RAP. Figure 9 demonstrates the effectiveness of those enhancement.

Generating Background RAP Flow: Once the RAP textured surface has been rendered, we texture the background with RAPs such that the direction of background flow is opposite to that of the surface across silhouette pixels. In other words, the background is just treated as another region in the image plane whose boundary is the silhouette of the surface from the viewpoint. The background field is generated, again, by setting up and solving a constrained optimization similar to Equation 1, with the following difference: the field generation is conducted in the image plane instead of on the surface. Given a viewpoint, the salient curves will be sampled in the image space, and the projected eigenvectors at these sample points will be used as the boundary conditions to the Laplace equation to generate a vector field directly. We have found that by generating a background field that respects salient features in the surface, illusion effect is more enhanced than using a background field that is unrelated to the surface, such as a constant directional field. To place RAPs in the background, we tessellate the background as brick pattern and texture each quad with a RAP such that the orientation of the RAP follows the direction of the underneath pixel. The contrast between the projected foreground surface and the background can be further enhanced by assigning different and complementary color combination of RAP.

Incorporating Shading and Unsharp Masking: Shading is an effective way of conveying shape. However, if we simply treat RAPs as a texture which we modulate with a Phong shading model, excessive shading can change the lightness of RAPs and reduce the strength of the illusory motion. In order to add shading effect without lost the motion illusion, we adopt a modified Gooch shading [8], which uses cold to warm colors to enhance the shading without change the lightness in a repeat asymmetric lightness order. Our approach is to modulate the yellow color in the four-color RAPs in our setting by rotating the chroma of the yellow along the L axis in CIELAB color space. The degree of rotation is determined by the intensity from Phong shading model. Brighter pixels will be rotated closer to the warm color; while darker pixels will be rotated more toward to the cold color. This approach can enrich the colorfulness of the result without sacrificing the strength of illusion. To further enhance the perception of shapes, we borrow the method of Luft et al. [20] in which they apply the unsharp masking filter to the depth image to increase the contrast across the boundary of the geometry.

5 Results

We now demonstrate our approach with a number of examples in Figure 9. More examples can be found in the supplementary materials. In all examples, we adopt the algorithm of Yoshizawa et al. [31] for fast and robust detection of crest lines on meshes. In addition, the user can edit/remove these crest lines or add new lines as constraints for flow generation. Given an quad-mesh as well as the constrained lines and selected RAPs, the image is then generated automatically. Readers are encouraged to view these results

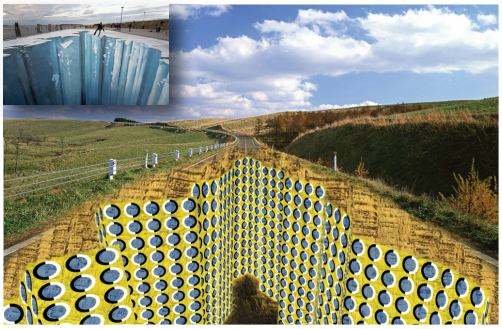

Fig. 6 The left top figure is "The Crevasse" by M*ü*ller (2008), and we apply his design style to "Street art with illusory motion" by proposed method.

by enlarging them on the display. To perceive stronger motions, glance around the images and avoid fixing the gaze onto a small area for longer than six seconds. Figure 3 compares results on the same model without view-dependent flow adjustment (c) and with such adjustment (d). Observe that the illusory motion perceived in (d) is stronger than in (c). Figure 9 demonstrates the effects of adding background RAPs and incorporating shading and unsharp masking (Section 4.3). In the first row, we use a TYPE IIa RAP as the surface texture, and show the enhance result with unsharp masking boundary and opposite background flow. In the second and third row, two new quad-like 3D RAPs are used to tile the surface, and enhance by the proposed modified Gooch shading, boundary and background.

Figure 7 provides two cases that demonstrates a limitation of the approach of [2] for illusory toon-shading. While their method can also be used for shape perception, it does not invoke illusory motions on surfaces. In addition, it cannot be used to visualize vector and tensor fields on surfaces. In our method, the focus is on surfaces rather than the background plane. We refer the readers to Figures 1 and 3 for a comparison with Figure 7.

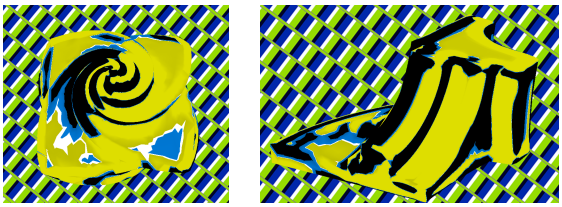

Fig. 7 Two cases showing the limitation of the approach by [2] for illusory toon-shading.

Our method can also be incorporated into texture-based vector and tensor field visualization techniques [1,30,29,32]. Figure 10 compares results on the same model using the RAPs only (a) and RAPs combined with Line Integral Convolution (LIC) method [1] (b) for visualizing vector fields on 3D surfaces. The illusory motion can help enhance these techniques by indicating the direction of the vector field as well as conveying the dynamic nature of the induced flow. We wish to emphasize that our approach is not aimed at replacing for existing visualization methods. Rather, it is meant to be an enhancement. In addition to illusory surface, we also integrate our technique into "Street Art", which often refers to popular painting in the public space. In left top of Figure 6 is a famous painting that is produced by "Edgar M*ü*ller". We use our illusory surface blend with texture to simulate the crevasse on the street as well, such as the Figure 6 shown.

User Study: Illusory motion would give different visual experience, such as flow motion, motion strength...etc, for different persons. Thus, the user study is necessary and it could help us to evaluate the visual experience for each illusory image, which are produced by proposed method. In our experiment, we have eight images from Figure 9 and Figure 10 and the 48 participants would join this user study. For each participant, they would mark the position and direction of spots where he/she can perceive the illusory motion. In the statistics data, the number of markers for each participant is 5.65 in average in Table 1. We visualize all collected data as spot map to see where evoke illusion is in high frequency. We also visualized the direction user perceived as green line. The results show the marked directions are almost the same among the different users, and the average angle between between direction the user perceive and actual line field is 22.66 degree. As study in [13], 5% of people cannot perceive motion illusion evoked by RAPs. It is very encouraging that our results evoke illusory motion among the most of participants. Figure 8 shows two spot maps generated from the user study and more examples can be found in our supplementary materials. According to the result of user study, it indicates that the proposed method is impressive for illusory motion and depicts the flow on the surface for the most of participants.

Limitations: The major limiting factor on the perceived motion is the size of the individual RAP elements in the image space. When they are outside the appropriate range of sizes, i.e., too large or too small, the resulting motion weakens or vanishes. Therefore, our method may not be self-sufficient when exploring such motion flows to describe finer details of 3D shapes. We also suggest to watch the figures in our supplementary materials, each page contains a single result, and enlarge them to full screen. Glancing around the images, without staring at a fixed position, also helps to perceive the effect. In our experiment, the best viewing distance to screen is roughly the half width of screen. Fortunately, some applications such as technical illustration are not aimed at depicting shapes in fine details and usually discard unnecessary geometric details for effective visual communication. An-

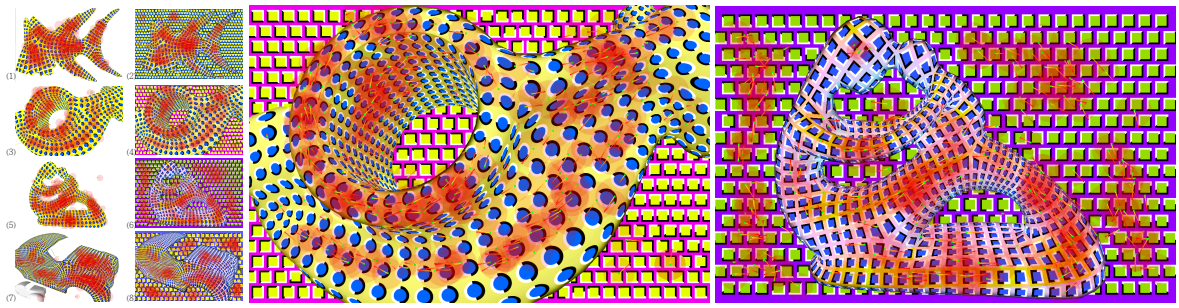

Fig. 8 Spot map from user study. Red spot is pointed out by participants, and green line indicates the direction user perceived. The more spots users select means that the evoke more illusory motion. Left image shows the all results in user study. In middle and right, these large images show more user study detail.

Table 1 Statistics and comparison of proposed vector-based representation

	(1)	(2)	(3)	(4)	(5)	(6)	(7)	(8)	average
Total marker	307	264	322	314	275	285	204	197	271
Average marker per user	6.4	5.5	6.7	6.5	5.7	5.9	4.3	4.1	5.65
Average angle error	23.12	25.19	17.6	16.87	20.67	22.27	26.68	29.19	22.66

other limiting factor is the quality of the input mesh, such as its regularity, amount of distortion, and number of extraordinary vertices. Also, by requiring quad-mesh as the input, our method cannot be directly applied to most 3D meshes without the remeshed processing.

6 Conclusions

Illusory motion is a fascinating physiological and psychological phenomenon. The motion effect on surface highly depends on several special conditions according to pattern placement and flow field design. In this paper we have presented a first approach to generate illusory motions on 3D surfaces. Using such motion cues for surface illustration and vector field visualization on surfaces are demonstrated. The user study also reveal the region of interest which people perceive most illusion effect. In the future we wish to extend our method to triangular meshes. Furthermore, we plan to investigate more direct ways of visualizing tensor, 4-RoSy, and 6-RoSy fields. Is it possible to produce gaze-dependent flows from static media? Can stereographic display be incorporated into the framework and what additional benefits can be gained by doing so? Finally, we wish to explore the use of other types of illusory motions and apply them to graphics applications.

Acknowledgements This work is supported by the National Science Council, Taiwan under NSC-102-2221-E-004 -008, NSC-102-2221-E-011-130, NSC-100-2221-E-006-188-MY3 and NSC-100-2628-E-006-031-MY3.

References

1. Cabral, B., Leedom, L.C.: Imaging vector fields using line integral convolution. In: Proceedings of ACM SIGGRAPH 1993, pp. 263–270. ACM Press / ACM SIGGRAPH, New York, NY, USA (1993)
2. Chi, M.T., Lee, T.Y., Qu, Y., Wong, T.T.: Self-animating images: illusory motion using repeated asymmetric patterns. In: SIGGRAPH '08: ACM SIGGRAPH 2008 papers, pp. 1–8. ACM, New York, NY, USA (2008)
3. Conway, B.R., Kitaoka, A., Yazdanbakhsh, A., Pack, C.C., Livingstone, M.S.: Neural basis for a powerful static motion illusion. J. Neurosci. **25**(23), 5651–5656 (2005)
4. DeCarlo, D., Finkelstein, A., Rusinkiewicz, S., Santella, A.: Suggestive contours for conveying shape. In: ACM SIGGRAPH 2003 Papers, SIGGRAPH '03, pp. 848–855. ACM, New York, NY, USA (2003)
5. Foley, J., van Dam, A., Feiner, S., Hughes, J.: Computer Graphics: Principles and Practice. Addison-Wesley (1996)
6. Garland, M., Heckbert, P.S.: Surface simplification using quadric error metrics. In: SIGGRAPH '97: Proceedings of the 24th annual conference on Computer graphics and interactive techniques, pp. 209–216. ACM Press/Addison-Wesley Publishing Co., New York, NY, USA (1997)
7. Girshick, A., Interrante, V., Haker, S., Lemoine, T.: Line direction matters: an argument for the use of principal directions in 3d line drawings. In: NPAR '00: Proceedings of the 1st international symposium on Non-photorealistic animation and rendering, pp. 43–52. ACM, New York, NY, USA (2000)
8. Gooch, A., Gooch, B., Shirley, P., Cohen, E.: A non-photorealistic lighting model for automatic technical illustration. In: SIGGRAPH '98: Proceedings of the 25th annual conference on Computer graphics and interactive techniques, pp. 447–452. ACM, New York, NY, USA (1998)
9. Gossett, N., Chen, B.: Self-animating line textures. Tech. rep. (2004)
10. Hertzmann, A., Zorin, D.: Illustrating smooth surfaces. In: SIGGRAPH '00: Proceedings of the 27th annual conference on Computer graphics and interactive techniques, pp. 517–526. ACM Press/Addison-Wesley Publishing Co., New York, NY, USA (2000)
11. Inglis, T.C., Inglis, S., Kaplan, C.S.: Op art rendering with lines and curves. Computers & Graphics **36**(6), 607 – 621 (2012)

12. Judd, T., Durand, F., Adelson, E.H.: Apparent ridges for line drawing. ACM Trans. Graph. **26**(3), 19 (2007)
13. Kitaoka, A.: Trick Eyes Graphics. Tokyo: Kanzen (2005)
14. Kitaoka, A.: Anomalous motion illusion and stereopsis. Journal of Three Dimensional Images (Japan) **20**, 9–14 (2006)
15. Kitaoka, A., Ashida, H.: Phenomenal characteristics of the peripheral drift illusion. VISION (Journal of the Vision Society of Japan) **15**, 261–262 (2003)
16. Kolomenkin, M., Shimshoni, I., Tal, A.: Demarcating curves for shape illustration. In: ACM SIGGRAPH Asia 2008 papers, SIGGRAPH Asia '08, pp. 157:1–157:9. ACM, New York, NY, USA (2008)
17. Lee, Y., Markosian, L., Lee, S., Hughes, J.F.: Line drawings via abstracted shading. In: ACM SIGGRAPH 2007 papers, SIGGRAPH '07. ACM, New York, NY, USA (2007)
18. Lefebvre, S., Hoppe, H.: Appearance-space texture synthesis. In: SIGGRAPH '06: ACM SIGGRAPH 2006 Papers, pp. 541–548. ACM, New York, NY, USA (2006)
19. Li, Y., Bao, F., Zhang, E., Kobayashi, Y., Wonka, P.: Geometry synthesis on surfaces using field-guided shape grammars. IEEE Transactions on Visualization and Computer Graphics **17**, 231–243 (2011)
20. Luft, T., Colditz, C., Deussen, O.: Image enhancement by unsharp masking the depth buffer. ACM Transactions on Graphics **25**(3), 1206–1213 (2006)
21. Lum, E., Stompel, A., Ma, K.L.: Kinetic visualization. IEEE Transactions on Visualization and Graphics **9**(2), 115–126 (2003)
22. Palacios, J., Zhang, E.: Rotational symmetry field design on surfaces. ACM Trans. Graph. **26**(3), 55:1–55:10 (2007)
23. Palacios, J., Zhang, E.: Interactive visualization of rotational symmetry fields on surfaces. IEEE Transactions on Visualization and Computer Graphics **17**, 947–955 (2011)
24. Potmesil, M., Chakravarty, I.: Modeling motion blur in computer-generated images. SIGGRAPH Comput. Graph. **17**(3), 389–399 (1983)
25. Ray, N., Li, W.C., Lévy, B., Sheffer, A., Alliez, P.: Periodic global parameterization. ACM Trans. Graph. **25**(4), 1460–1485 (2006)
26. Turk, G.: Texture synthesis on surfaces. In: Proceedings of the 28th annual conference on Computer graphics and interactive techniques, SIGGRAPH '01, pp. 347–354. ACM, New York, NY, USA (2001)
27. Wei, L.Y.: Visualizing flow fields by perceptual motion. Tech. Rep. MSR-TR-2006-82, Microsoft Research (2006)
28. Wei, L.Y., Levoy, M.: Texture synthesis over arbitrary manifold surfaces. In: SIGGRAPH '01: Proceedings of the 28th annual conference on Computer graphics and interactive techniques, pp. 355–360. ACM, New York, NY, USA (2001)
29. van Wijk, J., J.: Image based flow visualization for curved surfaces. In: VIS '03: Proceedings of the 14th IEEE Visualization 2003 (VIS'03), p. 17. IEEE Computer Society, Washington, DC, USA (2003)
30. van Wijk, J.J.: Image based flow visualization. In: SIGGRAPH '02: Proceedings of the 29th annual conference on Computer graphics and interactive techniques, pp. 745–754. ACM, New York, NY, USA (2002)
31. Yoshizawa, S., Belyaev, A., Seidel, H.P.: Fast and robust detection of crest lines on meshes. In: SPM '05: Proceedings of the 2005 ACM symposium on Solid and physical modeling, pp. 227–232. ACM, New York, NY, USA (2005)
32. Zhang, E., Hays, J., Turk, G.: Interactive tensor field design and visualization on surfaces. IEEE Transactions on Visualization and Computer Graphics **13**(1), 94–107 (2007)

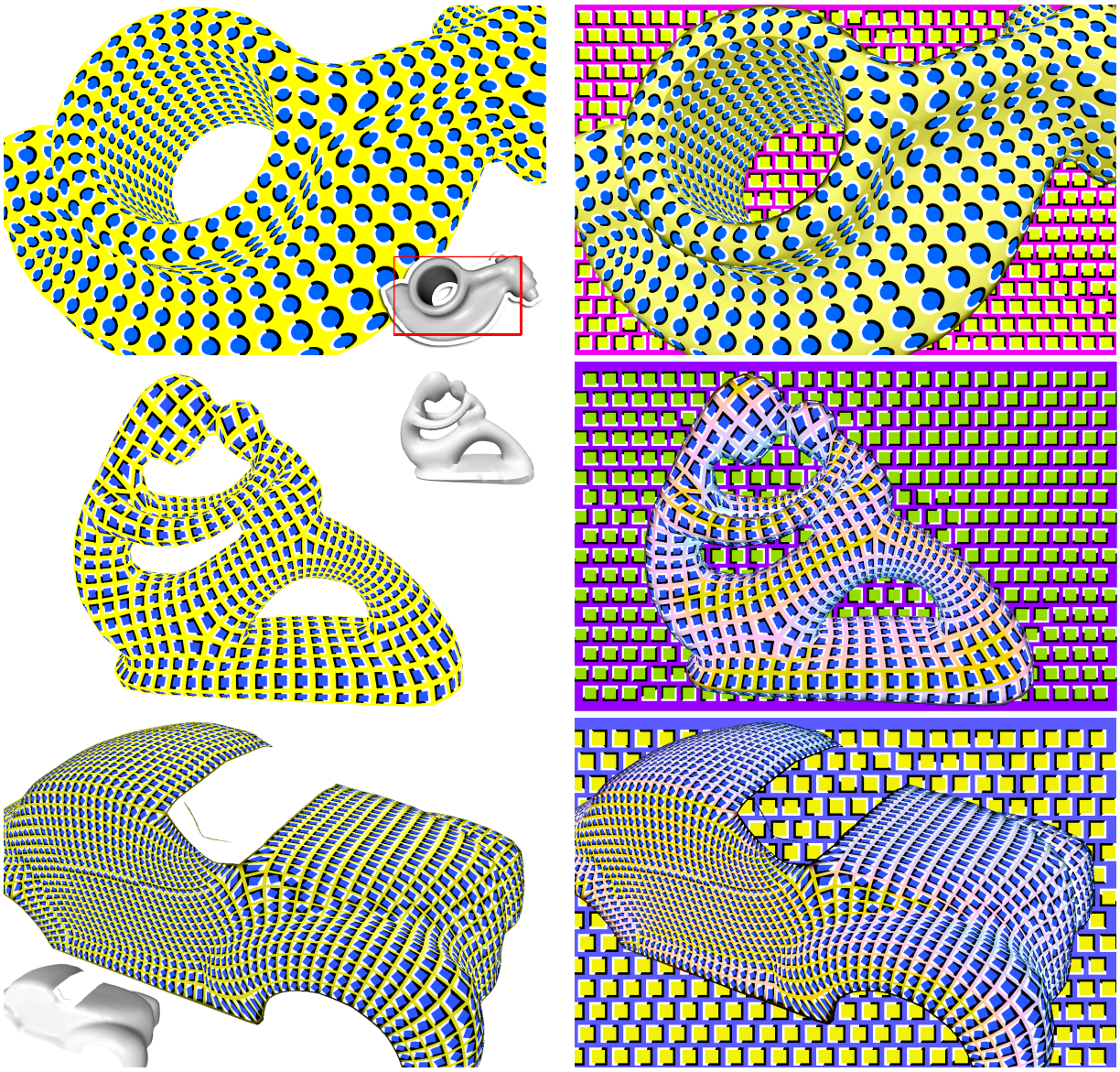

(a) (b)

Fig. 9 This figure demonstrates the enhancing effects: (a) RAP textured-models; (b) shading, image enhancement and the background are applied to (a).

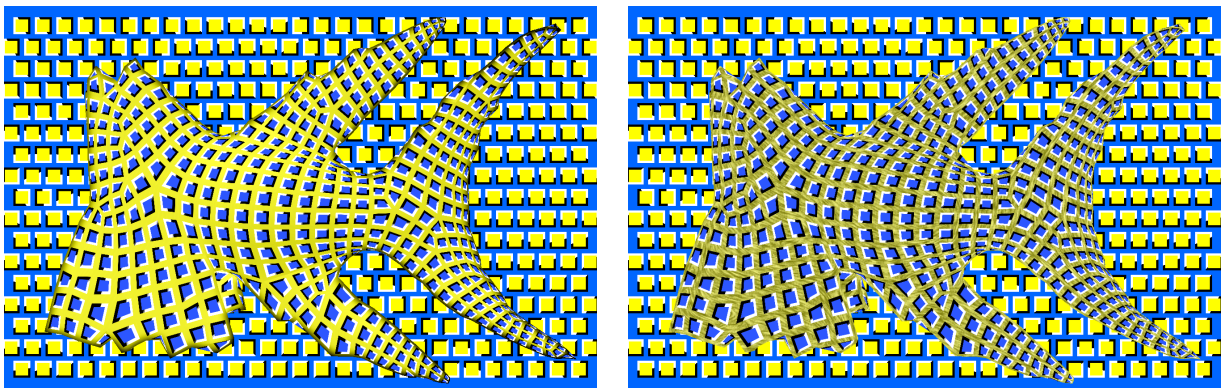

(a) (b)

Fig. 10 Combination with LIC (a) RAPs only, (b) RAPs+LIC.